水 文 ・ 水 資 源 学 会 誌
J. Japan Soc. Hydrol. & Water Resour.
Vol. 11. No. 1 (1998)　　pp. 39-60

Evaluation of Surface Fluxes Over a Paddy Field in Tropical Environment: Some findings from a preliminary observation of GAME

熱帯環境にある水田の表面フラックスの評価：GAME予備観測で得られたいくつかの知見

Masatoshi AOKI[1]・Takahiro CHIMURA[1]
青木正敏・千村隆宏
(Faculty of Agriculture, Tokyo University of Agriculture and Technology)
東京農工大学農学部

Ken-ichi ISHII[2]
石井健一
(Division of Science and Technology of Regional Environments, Kyoto University)
京都大学大学院農学研究科

Ichirow KAIHOTSU[3]
開發一郎
(Department of Natural Environmental Sciences, Faculty of Integrated Arts and Sciences, Hiroshima University)
広島大学総合科学部

Takashi KURAUCHI[4]
倉内　隆
(Hydrology Division, Royal Irrigation Department)
王立潅漑局

Katsumi MUSHIAKE[5]・Toshiyuki NAKAEGAWA[5]
虫明功臣・仲江川敏之
(Institute of Industrial Science, University of Tokyo)
東京大学生産技術研究所

Nobuhito OHTE[2]
大手信人
(Division of Science and Technology of Regional Environments, Kyoto University)
京都大学大学院農学研究科

Panya POLSAN[4]
パンヤ　ポルサン
(Hydrology Division, Royal Irrigation Department)
王立潅漑局

Steve SEMMER[6]
スティーブ　セマー
(Atmospheric Technology Division, National Center for Atmospheric Research)
国立大気研究センター

Michiaki SUGITA[7]
杉田倫明
(Environmental Research Center, University of Tsukuba)
筑波大学水理実験センター

Katsunori TANAKA[2]
田中克典
(Division of Science and Technology of Regional Environments, Kyoto University)
京都大学大学院農学研究科

Osamu TSUKAMOTO[8]
塚本　修
(Faculty of Science, Okayama University)
岡山大学理学部

Tetsuzo YASUNARI[9]
安成哲三
(Institute of Geoscience, University of Tsukuba)
筑波大学地球科学系

A preliminary observation for the GEWEX Asian Monsoon Experiment (GAME) was carried out at one of the observation sites of GAME near Sukhothai, Thailand in the summer of 1996, in order to assess the performance of prototype stations for measuring surface fluxes and soil moisture as well as to evaluate relative merits of the methods of determining fluxes. The data sets from three observation systems yielded turbulence statistics and the surface flux values by applying the eddy correlation method, the bandpass covariance method, the Bowen ratio method, the profile method and the bulk method. Intercomparisons of the resulting values indicate that the turbulence statistics are of high quality but the algorithm for evaluating bandpass covariance needs further improvement. It was also found that an accurate evaluation of energy storage in water body is essential in the application of energy balance approaches at paddy field. Overall, all stations performed satisfactory during the experiment in a hot, humid environment. However, a better protection against a strong rainfall appears to be needed for long term observations in this area.

Key words: GAME, Surface flux, Soil moisture

アジアモンスーンエネルギー水循環観測研究計画(GAME)の予備的な観測が、地表面フラックスと土壌水分を測定するためのプロトタイプ自動気象ステーションの性能の評価といくつかのフラックス測定法の相互比較を目的に1996年の夏，タイ国スコタイ付近において行われた。使用された3つの観測システムで得られたデータに渦相関法，バンドパスコバリアンス法、ボーエン比法、プロファイル法、そしてバルク法を適用することで地表面フラックスが得られた。乱流統計量やフラックスの相互比較の結果，統計量そのものは正確に得られているものの，潜熱フラックス評価のためのバンドパスコバリアンス法のアルゴリズムには改良の余地があることが示された。また、熱収支的な方法を利用する場合，水田の水体の貯熱量変化の正確な評価が重要であることがわかった。全体としてステーションは短期間の高温度高湿度下の運用に満足のいくものであったが、長期運用のためにはこの地域特有の強い雨に対する備えが必要であることがわかった。

キーワード：GAME，地表面フラックス，土壌水分

I. Introduction

GEWEX (Global Energy and Water Cycle Experiment) Asian Monsoon Experiment (GAME) has been proposed and is being implemented in order to enhance our understandings on the role of Asian monsoon in the global climate system. Among the several approaches within the GAME, the deployment of automatic weather stations (AWSs) which are capable of measuring not only the basic meteorological variables such as the air temperature and rainfall but also the surface fluxes of radiation, momentum, heat and water vapor and other key variables for an

[1] Faculty of Agriculture, Tokyo University of Agriculture and Technology, Fuchu, Tokyo, Japan
東京農工大学農学部
[2] Division of Science and Technology of Regional Environments, Kyoto University, Kyoto, Japan
京都大学大学院農学研究科
[3] Department of Natural Environmental Sciences, Faculty of Integrated Arts and Sciences, Hiroshima University, Higashi-hiroshima, Japan
広島大学総合科学部
[4] Hydrology Division, Royal Irrigation Department, Bangkok, Thailand
王立潅漑局
[5] Institute of Industrial Science, University of Tokyo, Tokyo, Japan
東京大学生産技術研究所
[6] Atmospheric Technology Division, National Center for Atmospheric Research, Boulder, CO, USA
国立大気研究センター
[7] Environmental Research Center, University of Tsukuba, Tsukuba, Ibaraki, Japan
筑波大学水理実験センター
[8] Faculty of Science, Okayama University, Okayama, Japan
岡山大学理学部
[9] Institute of Geoscience, University of Tsukuba, Tsukuba, Ibaraki, Japan
筑波大学地球科学系

Table 1 Requirement for the surface measurement to be made within GAME

Measurement Site	Representative of the area of 10-50 km^2
Measurements and Products	
Fluxes	Sensible and latent heat, soil heat flux and momentum
Radiation	Four components of radiation balance and surface temperature
General meteorology	air temperature, humidity, air pressure, wind speed and direction, and soil temperature (2-3 depths)
Hydrology	soil moisture, precipitation, (snow depth)
Vegetation	height, (Leaf Area Index), (stomatal resistance)
Soil	Soil profiles, hydraulic conductivity, soil moisture curve, heat conductance, etc.
Others	- Manual observations of rainfall, etc. should also be collected whenever they are available at nearby meteorological/hydrologic station - Field log of observations/maintenance should be kept, preferably with photos.
Observation Interval and Averaging Period	
Fluxes, Radiation, and Meteorology	Continuous 30-60 minutes averages
Vegetation	Infrequent intervals should be acceptable as long as seasonal variations can be obtained.
Soil	One time observations per station, except for soil moisture
Methods and Accuracy	
Fluxes	Accuracy of 20 W/m^2 can be considered as preferred target. Method of deriving fluxes can be anything as long as the methods are described in details.
Meteorology and Hydrology	The same standard method employed in a country where the station is located should be used whenever possible.
Soil and Vegetation	More emphasis should be placed on the detection of time variation of the soil moisture at single site. Variability of soil moisture in an area should be studies in a separate, independent intensive observation. For the determination of physical/physiological properties of soil/vegetation, measurements by a single rover team visiting every site are preferable.
Measurement period	From 1997 through 1999/2000.

extended period to capture the seasonal and annual variations, is one of the challenging GAME sub-programs and is currently in preparation stage within the framework of GAME-AAN (Asian AWS network) project.

Of particular importance for the success of the AAN project is the establishment of a reliable AWS system which can measure relevant variables to determine the surface fluxes as well as related variables reliably in most natural conditions at a reasonable accuracy. Although the needed variables and accuracy depend on particular requirements of scientific purposes, it has been agreed among the participants of the workshop on the measurements of surface fluxes in GAME held in Tsukuba, Japan in October of 1996 as well as of the subsequent GAME domestic workshop held in December 1996 in Nagoya, that the measurements should include such items as basic meteorological and hydrologic variables, surface fluxes, soil moisture and underlying soil and vegetation information of the measurement site. Also discussed were the requirements for the location of a station and the method of standardization of measurement level and data archive. These are summarized in **Table 1**.

For the past two years, the AAN working group has reviewed relative strength and shortcoming of the existing AWS systems, and tested several of them. As a result, it has been determined to use a modified type of a PAM-flux station (Militzer *et al.*, 1995) developed by National Center for Atmospheric Research (NCAR) in several "warm" experimental areas such as China, Tibet, Mongolia and Thailand, while for the colder Siberia region, a specially designed station for the low temperature operation will be used.

Main modifications to the PAM station were the addition of a second level hygrothermometer, an infrared-thermometer, a four-component radiometer system, and a TDR (Time domain reflectmetry) soil moisture measurement system. The first two items were added in order to evaluate the possibility to determine the fluxes by alternative/additional methods other than the eddy correlation and bandpass covariance method, which are the primary methods of flux evaluation of the PAM-flux station (Horst and Oncley, 1995), in order to add more reliability and robustness to the long-term, continuous flux determination. A prototype PAM station was constructed for the GAME project in early 1996 by NCAR and has been subject to various tests by the GAME scientists. In the present paper, some of the findings from a test operation of this station and two other systems in a very hot and humid environment in Thailand are presented. The main purpose of the test was to evaluate the performance of the systems; however, there are several issues such as the methods of flux evaluation and soil moisture, which merit discussions in more general scientific areas of the flux determination and micrometeorological technology and thus they will be presented in this paper.

II. Experiment

1. Site

The experiment was carried out during a wet season from August 21 through 31 of 1996, in an unirrigated paddy field near Sukhothai, Thailand (17°03′54″N, 99°42′19″E, and altitude approximately 50 m ASL) as part of activities of GAME-tropics which is one of the regional study areas of GAME. The site has been designated as one of the principal measurement sites in Chao Phraya basin, the main experimental area of GAME-tropics, because of the importance of the rice paddy in this region. **Photos 1a** and **1b** illustrate the site and its surrounding area. In the beginning of the experiment, the field was essentially dry without the presence of standing water; however, after the rainstorm on August 25, the field became paddy with water depth around 20-30 cm, which gradually decreased toward the end of the experiment. Air temperature was around 30°C with relative humidity 60-80%.

The average vegetation height h and leaf area index LAI of the site were determined approximately as h=26cm and LAI=0.23. However,

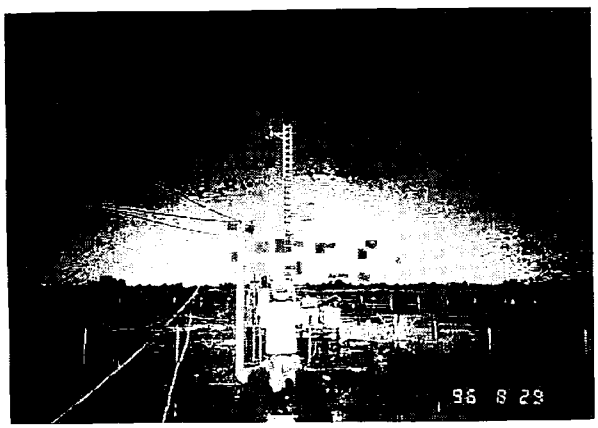

Photo 1a Experimental setup around the 10-m tower.

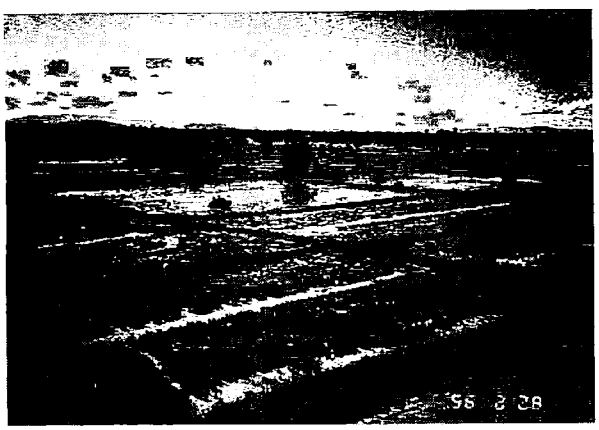

Photo 1b Surrounding area (View of the W-direction from the top of the 10-m tower).

within the section of 60 by 20 m where a 10-m meteorological tower was installed, the vegetation cover was less abundant than the surrounding area due to the effect of the tower construction in May-June. The surrounding area is a uniform paddy field and the fetch is estimated as at least several kilometers: however, there are isolated trees with height around 5-10 m present here and there in the area. In order to avoid the direct effects of such trees to the micrometeorological measurements, the nearest tree some 200 m away to the southwest direction was cut short down to 5 m.

The humic and laterite soil properties of the site were determined by taking soil samples of 100 cm^3 volume and by excavating an observation trench. Well-cultivated sandy soil was clearly observed from surface down to some 30 cm in the upper zone, and below that the laterite soil tends to dominate the soil column. **Table 2** summarizes the physical properties of the upper zone soil of the site. Unfortunately, those of the lower zone soil were not determined because of the difficulty for obtaining soil samples fully saturated with water.

Table 2 **Physical properties of the Sukhothai paddy site soils and the soil water contents at sampling in August, 1966**

Depth (cm)	Density (Dry:g/cm³)	Porosity (%)	Specific Gravity (g/cm³)
0-5*	1.50	36.5	2.53
0-5	1.75	33.0	2.61
5-10	1.78	29.5	2.53
17-22	1.73	33.1	2.59
0-22 (mean)	1.69	33.0	2.57

*Sample at the buried point of TDR-TRIME probes

2. Experiment setup

Three sets of measurement system were employed. The first one is the PAM-flux station for GAME, and will be referred to as PAM system in what follows. The 10-m mast specially designed for the station was not used in the experiment, since the 10-m tower was ready for use in the site (see Photo.1a). The four-component radiation system of PAM was not deployed, either, because it was under a separate test in Tohoku University at the time of the experiment. The details of the installed sensors and their heights are listed in **Table 3**. Most of the data were measured at 1-sec interval, with exceptions of the sonic anemometer and the bandpass hygrothermometer which were measured at 0.1 sec intervals, the TDR sensor (at 5-min. intervals), and the barometer (measured at 15 ms intervals internally and output the averages of the past 5 minuets every 5 minuets). All theses data were fed into the EVE (Environmental Variable Extractor, EVE) of the PAM station and recorded as processed data such as averages at 5-min. intervals and subject to the later analysis.

The second system (Aoki *et al.*, 1997) has

Table 3 Sensors of PAM system

		Height
Flux Measurement	- Sonic anemometer (ATI, SAT-211/3)	5.94 m
	- Hygrothermometer for Bandpass covariance method (NCAR)	5.94 m
	- hygrothermometer (NCAR)	2 and 9.5 m
	- Soil heat flux plate (REBS, HFT3)	-10 cm
	- net radiometer (REBS, Q7)	1.5 m
	- infrared radiation thermometer (Everest, 4000.4G)	2.0 m (looking toward E direction at 45 degrees view angle)
Meteorology	-Anemometer (R.M.Young, 9101)	9.5 m
	-Barometer (Vaisala, PTB220)	2.0 m
Hydrology	TDR Soil moisture sensor (TRIME, system)	-25, -55, -75, and -125 cm

Table 4 Sensors of BR system

Variables	Instrument	Height
Air and wet-bulb temperatures	Aspirated psychrometer with thermopile	9.5 m and 2 m
Soil temperature	thermistor sensor	- 1 cm
Water temperature	thermistor sensor	5 cm
Net radiation	net radiometer (EKO, MF40, modified)	1.5 m
Soil heat flux	soil heat flux plate	- 1 cm
Water level	pressure sensor	

been designed primarily to measure the surface energy balance through the determination of the Bowen ratio, and will be referred to as BR system. The sensors listed in Table 4 include sets of thermopile which should allow accurate determinations of temperature differences between two heights and between dry- and wet-bulb thermometers. Data are recorded as 10-minute averages.

The third system consists of a three dimensional sonic anemometer (Kaijo TR-90AH) and an infrared gas analyzer (Advanet Systems Inc., E009A), both installed at 5.94 m, the same height where the sonic anemometer of the PAM system was installed, to determine the sensible and latent heat fluxes directly through the application of the eddy correlation technique. This will be referred to as SA/IH system. The signals of three dimensional wind velocity, air temperature, and specific humidity q from these instruments were recorded on a PC through an A/D converter at a frequency of 10Hz. Each run consists of approximately 10 minutes and this was repeated every 15 minutes for most of the daylight period and some of the night time. In addition to these sensors, the raw data of the sonic anemometer of the PAM system were also recorded for comparison in the same manner with that used for the two sensors of this system.

Ⅲ. Methods of Surface Flux Evaluation

1. Profile method

The profile method for the flux estimation can be summarized as follows. In surface sublayer of the atmospheric boundary layer, the profiles of potential temperature and humidity are described by (1)-(2) on the basis of Monin-Obukhov similarity theory,

$$q(z_1)-q(z_2)=\frac{LE}{ku_*\rho l}\left[\ln\left(\frac{z_2-d}{z_1-d}\right)-\Psi_v\left(\frac{z_2-d}{L}\right)+\Psi_v\left(\frac{z_1-d}{L}\right)\right] \quad (1)$$

$$\theta(z_1)-\theta(z_2)=\frac{H}{ku_*\rho c_p}\left[\ln\left(\frac{z_2-d}{z_1-d}\right)-\Psi_h\left(\frac{z_2-d}{L}\right)+\Psi_h\left(\frac{z_1-d}{L}\right)\right] \quad (2)$$

where u_* the friction velocity, k von Karman's

constant, z the height above the ground, d the displacement height, θ the potential temperature, ρ the density of the air, c_p the specific heat of air ($\sim$1005 J kg^{-1}), L the Obukhov length, H the sensible heat flux, LE ($\equiv l \times E$) is the latent heat flux, l the latent heat for vaporization, and E is the rate of evaporation. The subscripts 1 and 2 refer to the measurement heights z_1 and z_2 within the surface sublayer. The symbols $\Psi_h(\ )$ and $\Psi_v(\ )$ denote stability correction functions for sensible heat and water vapor, respectively, and the formulations developed by of Businger and Dyer (e.g., Dyer, 1974, Businger, 1988, Högström, 1988) or those by Brutsaert (1992) can be used. For the values of u_*, those evaluated by the eddy correlation approach (see below) were used. The actual application of (1)-(2) to the data involves an iteration procedure bacase the equations are implicit, and details of the method can be found, for example, in Brutsaert (1982, p. 197-198) or Sugita (1996). The value of d was estimated as 2/3 of the average vegetation height. This method was applied to the data sets of PAM system.

2. Bowen ratio method

The energy balance equation of a layer near the surface, can be given by

$$R_n = H + LE + G + \partial S/\partial t \qquad (3)$$

where R_n is the net radiation, G is the soil heat flux, and $\partial S/\partial t$ the rate of change of energy storage in the layer, if the terms for advection and for photosynthesis can be assumed negligible. The upper boundary of the layer can be taken as the height where R_n was measured, and the lower boundary corresponds to the interface between the soil and the bottom of the pond of water in the rice paddy. The storage term $\partial S/\partial t$ was determined from the time variations of water temperature and water depth measured at a single location by BR system. For the application of (3), the direct measurements were made of R_n, while G was evaluated by using the data from a soil heat flux plate and those from the soil moisture and temperature measurements in the case of PAM. For the BR system, measurements made by the soil heat flux plate buried near the surface was assumed to represent G values.

The ratio of H and LE, i.e., the Bowen ratio B_0 can be defined directly from (1) and (2) by assuming $\Psi_h = \Psi_v$ as

$$B_0 = \frac{H}{LE} = \frac{c_p}{l}\frac{\theta(z_1)-\theta(z_2)}{q(z_1)-q(z_2)} \qquad (4)$$

Combination of (3) and (4) yields (5) and (6) which can be used to evaluate H and lE.

$$H = \frac{B_0}{1+B_0}(R_n - G - \partial S/\partial t) \qquad (5)$$

$$LE = \frac{1}{1+B_0}(R_n - G - \partial S/\partial t) \qquad (6)$$

This method was applied to the data sets from PAM and BR system.

3. Bulk method

The temperature profile equation for surface sublayer (2) can also be expressed by

$$\theta_s - \theta = \frac{H}{ku_*\rho c_p}\left[\ln\left(\frac{z-d_0}{z_{0h}}\right) - \Psi_h\left(\frac{z-d_0}{L}\right)\right] \qquad (7)$$

where θ_s is the surface temperature and z_{0h} the value of scalar roughness for sensible heat, which is the height where the temperature should be θ_s if the profile is extrapolated down to z_{0h}. For the application of (7) to determine surface flux H, it is necessary to know z_{0h} *a priori*. Although several models do exist to predict the value of z_{0h}, they are not without a problem, and it is probably best to calibrate the value locally whenever it is possible. For that reason, it was determined first from known values of H, u_* and $\theta_s - \theta$, by inverting (7) as,

$$z_{0h} = \exp\left(\left[\overline{\ln(z-d) - \Psi_h((z-d)/L)}\right] - \left[\overline{(\theta_s-\theta)}\, ku_*\rho c_p/H\right]\right) \qquad (8)$$

where the overbar denotes averaging over the height range of the surface sublayer. H values derived from the eddy correlation method (see below) with PAM data were used for this purpose. Once it has been determined as a constant or as a function of some variables which can readily be available, it should be possible to estimate surface flux H with (7). The data sets of PAM system were used to evaluate this

approach.

4. Turbulent flux determination

Eddy correlation method and bandpass covariance method were applied to the data sets of PAM and SA/IH system after the raw data were subjected to the pre-processing described in details in the appendix section.

1) Band-pass covariance estimate of latent heat flux.

The current configuration of the software in PAM/EVE is designed (Horst and Oncley, 1995) so that $(wq)_{bp}$, $(wt)_{bp}$, $(wt)_{hp}$ are evaluated for each 10-min. interval, where (wq) and (wt) represent the integrated cospectra of vertical wind speed and humidity or temperature within the frequency band specified by the subscript bp and hp. In practice $f_1 \leq f \leq f_2$ for bp and $f_2 \leq f$ for hp are used, where f_2 corresponds to the humidity sensor response time. Also, for the same 10-min. period, a linear regression between the wq- and wt-cospectra values within the band pass region of $f_1 \leq f \leq f_2$ is carried out and the values of regression constants A and B in $y=A+B\ x$ together with N, the number of cospectra combinations used to derive constants are recorded. In the current algorithm, the value of N is selected to have the maximum correlation coefficient, $r2$, in the 20 combinations of wq- and wt-cospectra data set. In the data used in this study, N value ranged between 3 to 20. $N=3$ was the indication of the scatter of the coepctra data set, and this often happens when the magnitude of flux is very small and under stable conditions. This problem has been remedied in the new algorithm of the bandpass covariance approach of PAM III by increasing the bandwidth used to determine the value of B (Horst *et al.*, 1997). Note that the above algorithm effectively assumes that the regression coefficient A is close to zero. This is not always the case, and could be a source of error in the evaluation of fluxes. This possible problem has also been fixed in the new algorithm.

Assuming the scalar similarity of the water vapor and sensible heat for $f_1 \leq f$, the $(wq)_{hp}$ can be derived as

$$(wq)_{hp}=(wt)_{hp} * B \tag{9}$$

Then the total covariance wq is evaluated as follows,

$$wq=(wq)_{bp}+(wq)_{hp} \tag{10}$$

and the latent heat flux can be evaluated as,

$$LE=\rho \times l \times wq \tag{11}$$

2) Eddy correlation method

With the availability of fast response sensors for wind speed and temperature, the turbulent fluxes can be obtained directly by applying the eddy correlation technique given as follows.

$$\tau=-\rho \times \overline{uw} \tag{12}$$

$$u_*=\sqrt{-\overline{uw}} \tag{13}$$

$$H_s=\rho \times c_p \times \overline{wt} \tag{14}$$

where τ is the momentum flux, H_s the sonic sensible heat flux, which includes the effect of humidity contribution (Kaimal and Gaynor, 1991). This contribution can be removed by

$$H=H_s-0.06LE \tag{15}$$

in which LE from (11) can be used. The procedure to apply the eddy correlation method with the data from PAM and those from SA/IH system is essentially the same and (13)-(15) were used after needed pre-processing to determine the u_* and H values. In addition, with the data from SA/IH system it is possible to determine the fluxes of latent heat and CO_2 by applying the eddy correlation technique, given as,

$$LE=l\rho \times wq \tag{16}$$

$$F_c=\overline{wc} \tag{17}$$

where F_c and c represent the flux and fluctuation of CO_2, and $\overline{wc}$ represents covariance of w and c for the region $f_1 \leq f$. In order to obtain reliable fluxes by (16)-(17), the outputs of the infrared gas analyzer need to be calibrated. This was carried out in the laboratory shortly after the experiment, by measuring values of c and q both with Advanet E009A and with a closed-path infrared gas analyzer (LiCor Inc., LI6262) which itself was calibrated by the standard gas beforehand, and by comparing the outputs. Finally, the technique proposed by Webb *et al.* (1980) was applied, to correct latent heat flux and F_c values

evaluated from (16) and (17) in order to account for the changes in the density of air associated with simultaneous transfer of latent and sensible heat. Note, however, the correction to the latent heat flux by this technique is very small and might as well be ignored.

Ⅳ. Method of Soil Moisture Detection

The time domain reflectmetry (TDR) principle (Topp. *et al.*, 1980) of the transverse electric and magnetic (TEM) wave was employed for the determination of soil water content. In practice a TRIME device (IMKO GmbH, type MUX-6) based on the TDR method was used in this observation. The TRIME measurement of the TDR-pulse is realized by direct time measurement, instead of indirect voltage measurements (Stacheder, 1996). The reflected pulse voltages that indicate the electric conductivity of soil water were also measured by this device at the time of the soil moisture measurement. Four TRIME probes of the two-rod type were installed horizontally at 25 cm, 55 cm, 75 cm, and 125 cm depths on May 15, 1996. The used probes (type P2Z at 125 cm depth and P2 at other depths) have two rods with the 1.5 cm spacing and the 10 cm length and the effective measurement area of the probe is an ellipsoid with the 3-6 cm apse line length and the 1.5-3 cm minor axis length around the rods. The probes were factory calibrated based on the

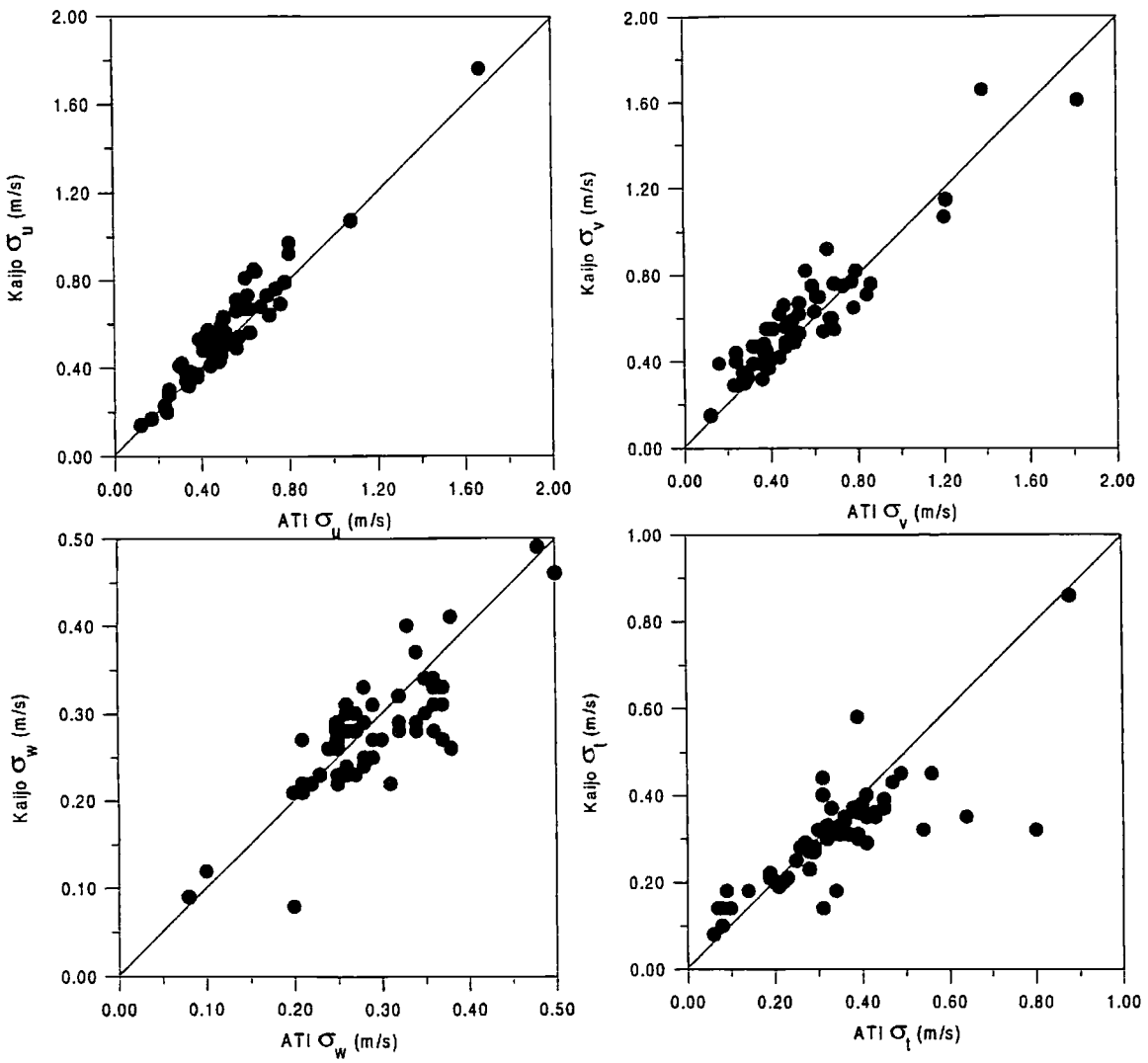

Fig. 1 Comparison of the standard deviation σ of u, v, w, and t measured from the Kaijo sonic anemometer of SA/IH system and the ATI sonic anemometer of PAM system

method of Topp. *et al.* (1980) at more than 10 points within the volumetric water content range of 0-100% with a mineral soil column. Data were collected at 5-min. interval during the test period from the 26th to the 31st in August, 1996. In addition, the water table depth of the unconfined groundwater was measured periodically using a metal tape scale around the experimental site.

V. Flux Evaluations

For the purpose of flux evaluation, the data observed on two days of August 28-29 when the surface was ponded with water body, and some data from August 22 when the surface was dry were used.

1. Turbulent determination of flux with PAM system.

Because the algorithm of the bandpass covariance method currently employed by the PAM system still needs improvement in terms of both its practical application procedure and the theoretical basis, it is probably best to check the performance of this method against that of more reliable approaches. This was carried out by comparing turbulence statistics. **Figures 1-2** illustrate comparison of the statistics. u, v, w, t, and uw measured by the ATI sonic anemometer of PAM and the Kaijo sonic anemometer of SA/IH system. The agreement can be considered, in general, quite good, except for some outlier points, especially that found in u, v, and w comparisons, despite the fact that two sonic anemometers were separated horizontally by approximately 1-1.5m. This clearly indicates the reliability of the two sonic anemometers used in the measurements. **Figure 3** shows a similar comparison of the latent heat fluxes evaluated by the eddy correlation method (16) and by the bandpass covariance method (10)-(11). The eddy correlation fluxes derived with PAM sonic denoted by the closed circles tend to be smaller than those from SA/IH sonic. The exact cause(s) of this difference is not clear, but the underestimation of fluxes by the combination of the ATI sonic anemometer of PAM with the SA/IH gas analyzer, due to the sensor separation is suspected. During the experiment, the SA/IH sonic anemometer and the gas analyzer were installed side by side, while the PAM sonic anemometer

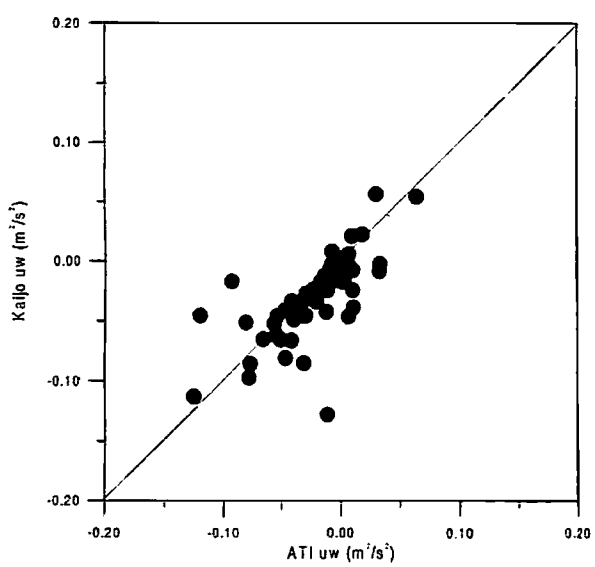

Fig. 2 Same as Fig. 1 but for the covariance uw

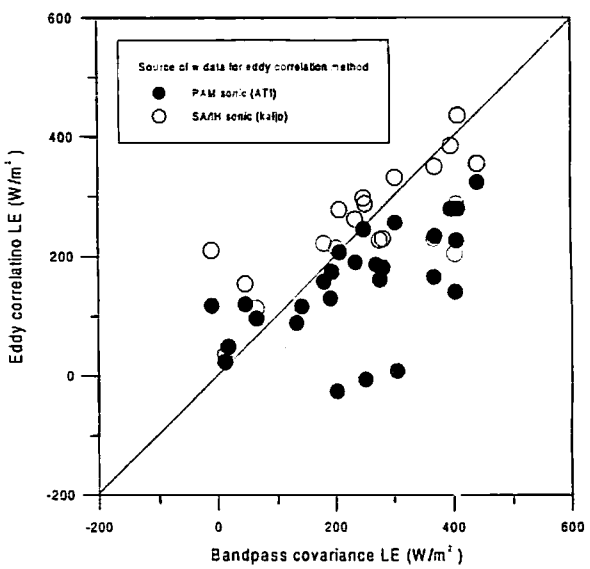

Fig. 3 Comparison of the latent heat fluxes LE evaluated by eddy correlation method (16) with the data from the Kaio/ATI sonic anemometers and the infrafed gas analyzer and those from bandpass covariance method (10)-(11) with the data of the ATI sonic and the bandpass covariance hygrometer of PAM system

and the SA/IH gas analyzer had a horizontal distance of some 1-1.5m. Although there are some uncertainties remained on this issue, the LE fluxes from closely located instruments of SA/IH system may be judged more reliable. The comparison between the LE values derived from the bandpass covariance method and those from the eddy correlation technique with the SA/IH system, indicates a fair agreement. This probably reflects the validity and usefulness of the bandpass covariance method. However, the scatter of the data points and the presence of some outlier points clearly indicate the need for a better technique in the implementation of the bandpass covariance approach. Until such technique becomes available, it is probably a good idea to record all the 20 cospectra combinations so that a later thorough re-analysis can be possible.

2. Bowen ratio approach by BR system

Figure 4 illustrates the comparison of the Bowen ratio values, evaluated by SA/IH system and by BR system. In the former system, the Bowen ratio is calculated from fluxes of latent and sensible heat, both directly measured by the eddy correlation system. In the BR system, Bowen ratio was evaluated by (4). Those values derived from combination of the infrared SA/IH gas analyzer and the sonic anemometer of PAM system are also given for comparison.

The B_0 values from the BR system tends to be larger by some 45% than those from the SA/IH sonic anemometer and infrared gas analyzer, while the agreement is better between B_0 from BR system and those from PAM sonic anemometer and SA/IH gas analyzer. As noted above, the combination of the sonic anemometer and the hygrometer of the SA/IH system may be more reliable due to the closeness of the two sensors. However, the later examination of the BR system did not reveal any malfunction at the time of measurement. It is still possible that the eddy correlation values are the cause of the disagreement, since the measurements require complex operations. Thus the cause(s) this possible overestimation of the B_0 values by the BR system remain unsolved and it will need further investigation.

Figure 5 shows the individual comparisons of the fluxes of H and LE. The BR system tends to produce larger fluxes. In Figure 4, it was found that B_0 values from the BR system tend to be larger than those from SA/IH system by some

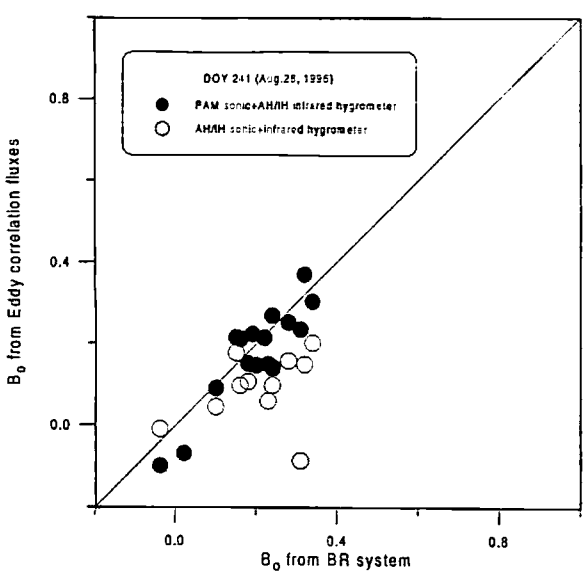

Fig. 4 Comparison of Bowen ratio values B_0 derived as the ratio of H and LE evaluated by (14) and (16), and those from (4)

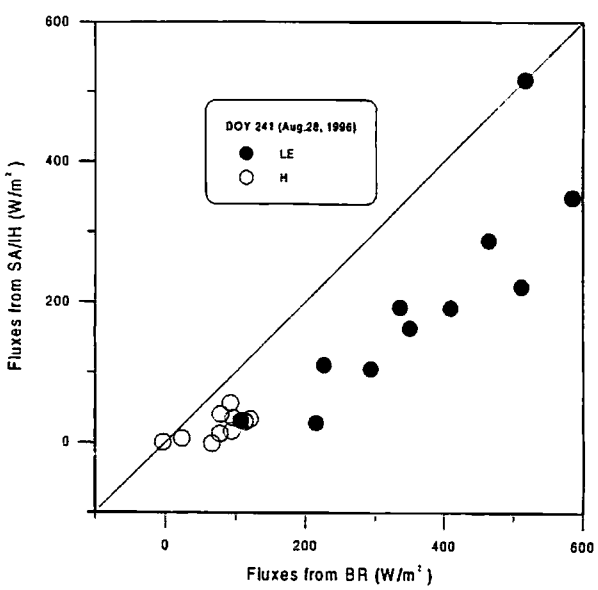

Fig. 5 Comparison of LE and H values from eddy correlation technique and those from Bowen ratio method

45%. Overestimation of B_0 values by 50% at B_0= 0.2 would produce underestimated LE fluxes by 8% and overestimated H fluxes by 35%. The additional variables introduced in this comparisons are R_n, G, and dS/dt, and the overestimated fluxes imply that either R_n was too large, or G and/or dS/dt value were too small.

R_n values measured by the BR system are found to be larger than those from PAM system by some 10% on average during daytime. Later investigations have revealed that this difference was caused by the difference of the calibration procedure by the two different manufacturers of EKO Instruments Trading Co., Ltd. (EKO) and Radiation and Energy Balance Systems, Inc. (REBS). Net radiometers were calibrated against a black body reference in the laboratory and also against a reference radiometer outside during nighttime at EKO, while REBS's procedure also involves field calibration against a reference radiometer during daytime. Thus the EKO's radiometer is calibrated for infrared wavelength only while the REBS's radiometer is also calibrated for shortwave radiation.

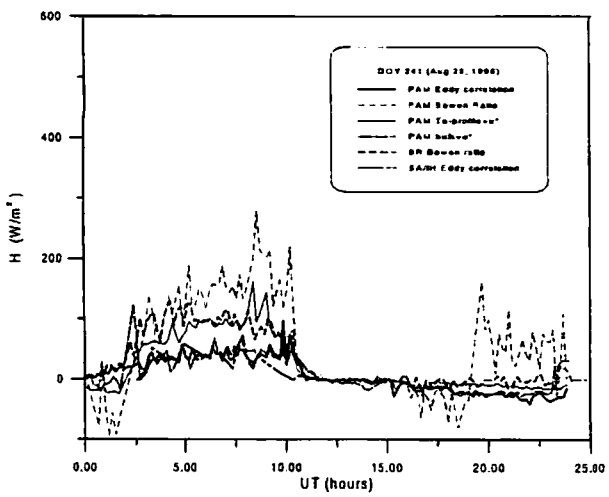

Fig. 6 Diurnal variation of H, evaluated by various methods on August 28. The techniques to derive fluxes and equipment used for the analysis are as follows. PAM eddy correlation: eddy correlation method with the ATI sonic anemometer of PAM, PAM Bowen ratio: Bowen ratio approach with two level measurements of temperature and humidity by PAM, PAM Ta-profile+u_*: the profile method with two level measurements of temperature by PAM together with u_* values determined by sonic anemometer of PAM, PAM bulk+u_*: the bulk method with IRT surface measurements and air temperature of PAM together with u_* values determined by sonic anemometer of PAM, BR Bowen ratio: Bowen ratio approach with two level measurements of temperature and humidity by BR system, and SA/IH eddy corelation: eddy correlation method with the Kaijo sonic anemometer and the Advanet gas analyzer of SA/IH system

G values from PAM tend to be larger than those from BR system during daytime typically by 20-40 W/m². Since careful check of both methods of observation and analysis did not reveal any problems, this difference appears to be the real difference between the two places where the sensors were buried. Clearly a better sampling strategy of G measurement is needed to get horizontally average value of G.

To further assess disagreement of fluxes, Figures 6 and 7 illustrate the diurnal variations of the latent and sensible heat fluxes. Although the general features of the comparisons are the same with those observed in Figure 5, one additional information can be derived from the diurnal variations. The fluxes from Bowen ratio method tend to come to the peak earlier than those from the eddy correlation approaches. This shift in the phase of the diurnal variation can only be caused

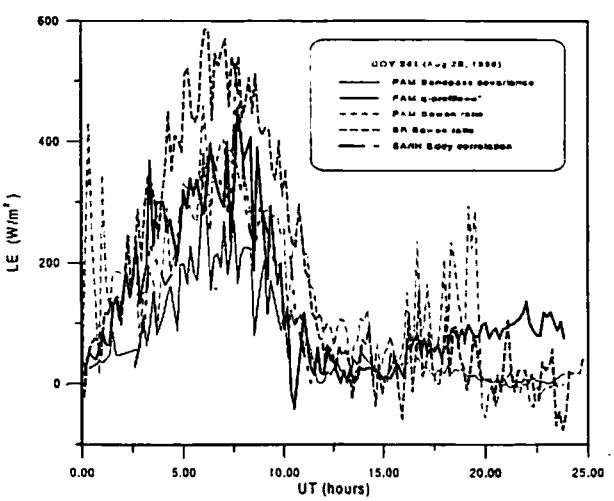

Fig. 7 Same as Fig. 6 but for LE

by the error in dS/dt. During the experiment, changes in the energy storage in water body was evaluated from a single measurement of water temperature and single measurement of water depth near the station. This was probably not sufficient to accurately determine the value of dS/dt. For example, a visual observation indicated that the soil surface was not flat but had micro-topographic features with the vertical variations at least of the order of ± 3 cm. Since the typical temperature increase/decrease during a daylight 10-minute period was approximately 0.4°C and since the water depth was of the order of 9 cm, the overestimation of water depth by 3 cm would result in the overestimation of the fluxes by some 80 Wm^{-2}. Also, the error of the water temperature of only 0.13°C would cause the error of the same magnitude. Clearly a better method to evaluate the storage term is needed. One possibility would be to adjust or "calibrate" the measurement of water depth at a single location so that it represents the area of interest. Alternatively, the measured values of water temperature could also be "calibrated" so that they represent the areal mean. In either case, it can be done if the rest of the energy balance components of R_n, H, LE, and G is known independently. Then the dS/dt values can be evaluated from (3) and the measured depth or temperature can be increased/decreased to produce proper values of dS/dt. However, a thorough investigation will be needed before this idea can become a practical tool.

In addition to the difficulty in the evaluation of dS/dt, there is additional issue to be considered. The values of R_n, G and dS/dt represent only a small area probably of the order of 10^{-1}-10^{1} m, while other atmospheric measurements such as variables measured by the sonic anemometers and air temperature reflect larger upwind area of 10^{1}-10^{2} m. This mismatch of the representative area of the measured variables can be another reason for the worse comparison of the fluxes.

3. Additional flux evaluation approaches with PAM data set

As noted above, PAM system consists not only of the sensors needed for the direct flux evaluation by the eddy correlation and bandpass covariance methods but also of the additional sensors for the profile method, Bowen ratio method and the bulk method. Although they are meant supplemental for the direct evaluation of the flux and for added reliability in the long term flux evaluation in GAME, the sensors consist of those of high standard which often are used in regular flux determination. Thus the comparison of the resulting fluxes with those from direct observations should give some idea of the reliability of such approaches.

Figures 6 and 7 illustrate the diurnal variation of the sensible and latent heat fluxes evaluated by these methods as compared with others. The profile method produced sensible heat flux that is too large and latent heat flux that is too small when compared against the fluxes from the eddy correlation method. The scatter plots (**Figures** 8 and 9) indicate that the sensible heat fluxes are overestimated systematically while in the latent heat flux estimation the error is more of a random

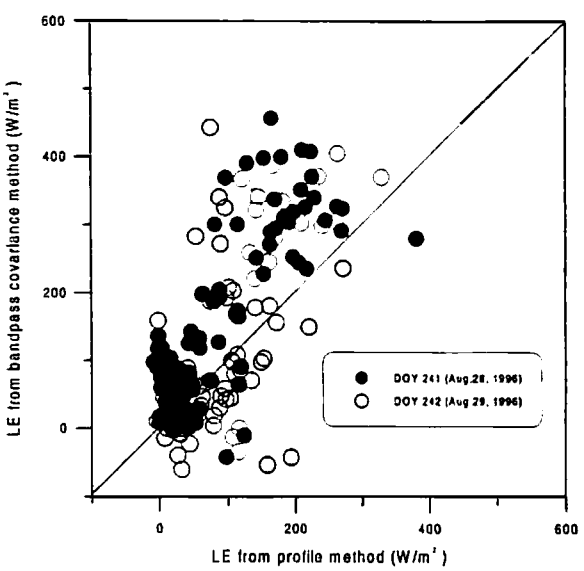

Fig. 8 Comparison of LE values from bandpass covariance method (10)-(11) and those from profile method with the PAM data

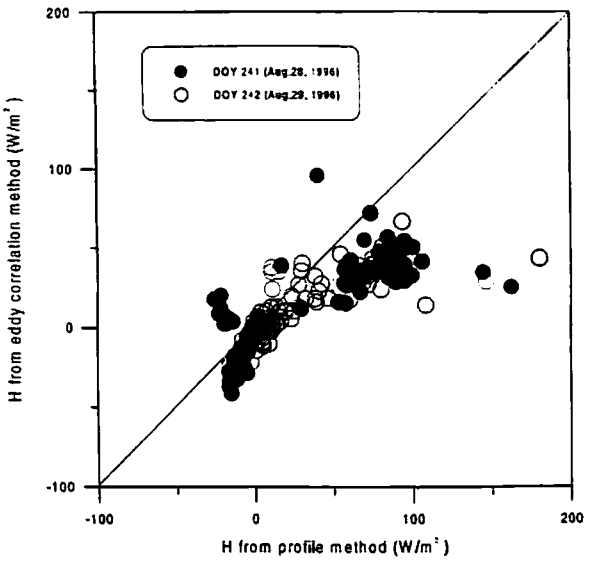

Fig. 9 Comparison of H values from eddy correlation method (14) and those from profile method with the PAM data

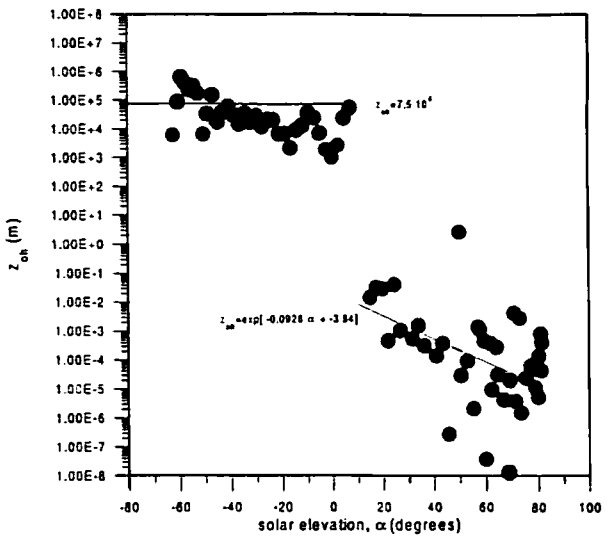

Fig. 10 Relation between z_{0h} derived by (8) and solar elevation. Negative solar elevation merely indicates nighttime. Also indicated are the regression line fitted to the daytime data and mean value for the nighttime data

nature. The systematic nature of the error of the sensible heat flux probably reflects the fact that temperature sensors in the identical radiation shield are more accurate and consistent than the relative humidity sensors. Possible reasons for the consistent overestimation of H by the profile method include that the fixed positioning of the two sensors failed to avoid the effect of the systematic difference of the two sensors. Another possible reason for the overestimation of the fluxes is the underestimation of the d value. If the d value was raised from $2/3h$ to h, for example, the fluxes would decrease by some 4%. However, the magnitude of the sensible heat flux was very small and can be close to the measurement error itself. Thus it is difficult to determine the exact reasons for the difference of H flux values. Yet, the consistent nature of the difference implies that the difference of air temperature at two heights should give valuable information on H fluxes.

Fluxes from the Bowen ratio approaches not only include the effects of systematic difference of the outputs of the two sensors at two levels but also the likely errors in the evaluation of R_n, G, dS/dt and thus the reliability of the resulting fluxes is somewhat questionable. The good agreement of the sensible heat fluxes from the bulk approach is not surprising as the key surface parameter, the scalar roughness for sensible heat, was calibrated locally and parameterized with the solar elevation during daytime and set to be a constant at night as shown in Figure 10 (for details, see also Sugita *et al.*, 1996). However, this gives an idea that as long as a periodic calibration of the surface parameters can be made, it should be possible to derive sensible heat fluxes reliably by the bulk method. This can be accomplished fairly easily with the present configuration of PAM station for GAME.

4. Variability of surface energy balance at paddy field

Figures 11 and 12 illustrate the diurnal variations of energy balance components on two days. On August 28, there was water present above soil surface, while on August 22, the field was essentially dry. The difference is quite significant between the two days as the changes in the energy storage dS/dt is the major energy balance component on Aug. 28 while there is no equivalent term on Aug. 22. Again, this clearly indicates the need

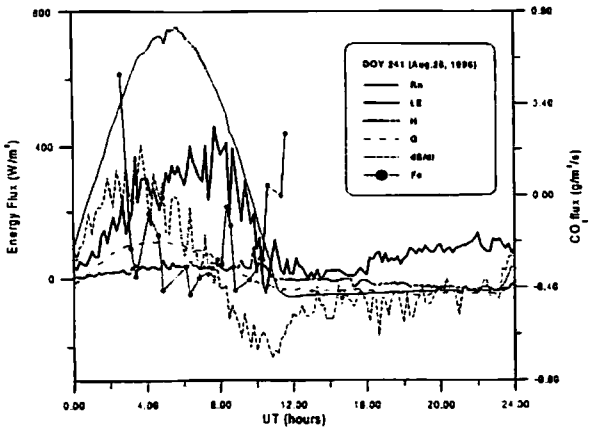

Fig. 11 Dirurnal variation of surface fluxes on August 28, with the presence of paddy water. *Rn* and *G* were from PAM system, *LE* from the bandpass covariance method with PAM data, *H* from the eddy correlation method with PAM data, and F_c from the eddy correlation method with SA/IH system data, and *dS/dt* from measurements of water temperature and water depth by BR system

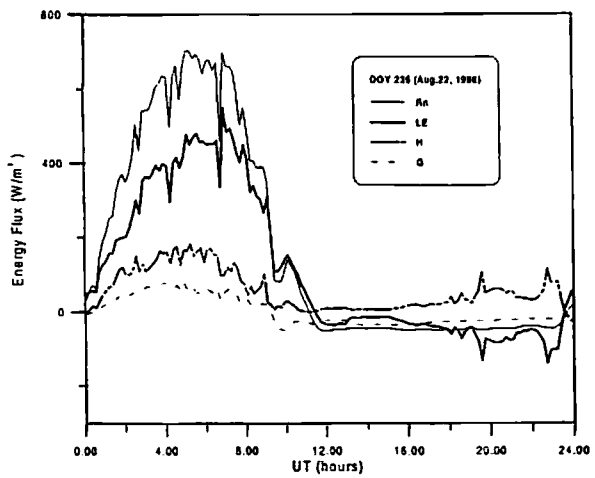

Fig. 12 Same as Fig. 11, but for August 22 when the field was dry. All components were measured and derived by BR system

for a better method to evaluate storage term of the energy balance at paddy site.

Note that in these two figures, the flux data from several different systems are used as indicated in the figure captions, mainly because of the lack of continuous, simultaneous measurements of all three systems. However, the general features and differences of the diurnal energy balance variations between two days as indicated in the figures remain the same even if other flux data are used.

VI. Soil Moisture

On August 25, the water table was at 25-30 cm depths and sporadic ponded water on the soil surface was observed. With the increased rainfall after August 26, the ponded water covered soil surface completely and the water table of groundwater started rising and reached to the soil surface on Aug. 28.

In general, the data acquisition was smooth and there was basically no trouble in the data logging and communications between PAM and TDR-TRIME during the test period. The raw data were processed by applying the moving average which produced one mean value out of four raw values. This pre-processing effectively eliminated the noise in the raw data below accuracy level of 2-3% of the TRIME system specified by the manufacturer (see below). The resulting time variations of the soil water content are shown in Figure 13. A fluctuation of the order of 2～5% can be seen and the magnitude of the fluctuation is clearly larger at high volumetric water content. This result suggests that the reproducibility and accuracy of the TDR-TRIME measurement become worse at high water content region. Also noticeable is the fact that the water content at all depths, and especially at 25 cm depth, decreases gradually toward the end of experiment. Since the soil was essentially saturated with water during the experiment, there should not be any change in soil moisture. Even if there had been unsaturated soil pores present down below, the observed rise of water table and heavy rainfall events should have resulted in gradual increase of soil moisture. Thus this gradual decrease in soil moisture observed by the TDR sensor is probably not real. A possible cause of this decrease is a slight, gradual reduction of pore space between the prove rods and surrounding soils. When the TRIME probe is first inserted into the soil, it is possible that there is a space

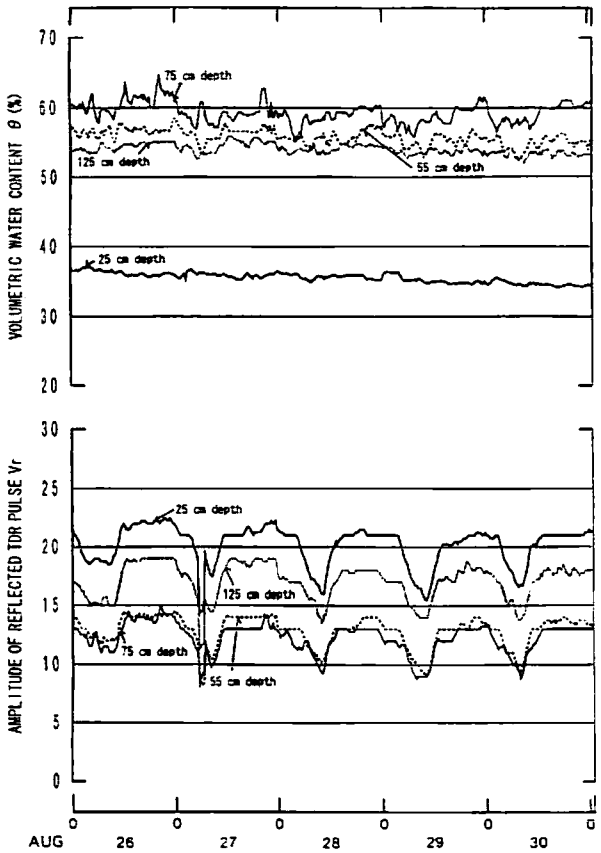

Fig. 13 Measurement results of the volumetric water content and the amplitude of the reflected TDR pulse voltage at 20-min interval. Time and date are given in *UT*

around the rods, which is filled with water in the saturated soil. With time, the soil gets settled, and the contact between probe rod and soil becomes better so that the resulting measurements of soil moisture content decreases. Another possible cause is the gradual dissolution of iron-rich soil material into the soil water and resulting increase in electric conductivity. Although it has been shown (e.g., Topp *et al.*, 1980, Dalton, 1984) that the salinity within soil did not affect the water content measurement by the TDR method in a wide range of electric conductivity (e.g., up to approximately 1 dS/m in the case of Dalton *et al.*, 1984), there is no *a priori* reason why it should not affect the water content measurements at higher salinity. Also different irons might cause different influences to the water content measurements at the same electric conductivity level. Although it is not very likely that the conductivity at the experimental sites is much higher than 1 dS/m, the possibility that it is indeed higher and it affects soil moisture measurements should be investigated.

The maximum and minimum values of the volumetric water content at 25 cm depth during the test period were 37% and 34.1%, respectively. The mean value can be obtained as 35.6% from these values. This is nearly equal to the mean value of the porosity of the soils at the 0～22 cm depths as listed in Table 1 and the difference is only 2.6%. This agreement implies that the accuracy of the soil moisture measurement in the low to middle range of the volumetric water content by TDR-TRIME is of the order of 2-3%, which also agrees with the specified accuracy of the P2 probe of±2% for 0-40% and±3% for 40-70% by the manufacturer.

Figure 13 also shows time change of the amplitude of the reflected TDR-pulse voltage. Small voltage value implies the high electric conductivity of the soil water. A glance at Figure 13 indicates that the voltage in the lower zone is smaller than that at 25 cm depth. This is reasonable because the laterite soil below is iron-rich (Goudie and Wilkinson, 1977) and is more electrolytic than that in the upper zone soils. The reflected pulse voltages of all depths decrease gradually with pronounced daily cycle during the observed period. Since there is no time lag in the diurnal changes at each depth, this daily cycle was probably caused by the temperature variation effects on a TDR-TRIME multiplexer box which encloses both a multiplexer part and electric circuit boards for signal processing. The box was placed in a PVC box under solar panels. Thus it might be a good idea to keep the multiplexer box in a place where temperature is less variable for more precise measurements of the electric conductivity. Note, however, that this precaution may not be necessary for the soil moisture measurement alone with the TRIME system, because the temperature effects on the soil moisture measurement is clearly very small

as observed in small diurnal variation of soil moisture; also, the coefficient of determination between the soil temperature and the TDR-derived water content was only 0.082. The gradual decrease of the voltage with time can probably be explained by gradual dissolution of iron-rich soil material into the soil water and resulting increase in electric conductivity. Another possible cause is the initial gradual reduction of the space between the sensor and soil materials as discussed above. However, a theory (e.g., equation (8) of Dalton *et al.* (1984)) predicts that decrease in soil moisture due to reduction in pore spaces should result in decrease in electric conductivity of the soil and thus should increase in the measured voltage. Thus this is not likely to be the cause of observed voltage decrease.

Ⅶ. General Performance of the Station in Hot, Humid Area

Evaluation of the overall performance of the three prototype stations is one of the purposes of the preliminary observation. In general, the stations were judged quite reliable even in hot, humid conditions. However, minor improvements are felt necessary to make more reliable, long-term measurements. One of such improvements is the protection against rainfall and humidity. Tropical rainfall is very intense and rainfall as heavy as 10 mm/5 min. was recorded during the experiment. The consequences of rainfall of this intensity is the water penetration into the sensors, cabling and connectors as well as into the data acquisition system. They could result in immediate failure of the system, although this was not encountered during the experiment. Less serious, but yet problematic consequences are the resulting corrosion of the connecters, cables and others. This was observed even after this short experiment period. Thus a better protection against rainfall is probably one challenge we must face in order to make reliable surface measurements over an extended time period.

Finally, the damages to the sensor as well as electronic system due to lightning is a possibility and a likely cause of a problem in this area. Although there is no ultimate solution to that, there are probably two remedies that should reduce the risks. One of them is the installation of lightning rod on the tower and good grounding of it. This was installed before the observation. Another strategy is not to use commercial electricity, which is susceptible to the lightning and which could act as the source of electric serge. During the experiments, two separate sources of electricity were examined, in addition to the commercial electric supply. The combination of six 64W solar panels with three 100AH batteries was found to work satisfactory to support PAM system which approximately consumes 26W of energy. Also a 60W propane generator was tested for the operation of PAM system and of BR system. Both worked without a problem.

Ⅷ. Concluding Remarks

Initial results of the GAME field measurements are presented. The results of the flux comparison indicate that the variables from two different sonic anemometers are quite reliable and resulting fluxes from eddy correlation methods also appear to be reliable. However, the bandpass covariance algorithm applied to the slower response humidity sensor is not quite satisfactory and it resulted in some unreasonable results. Clearly, the method of determination of the B value should be improved. Also, it was shown that for the application of the Bowen ratio method, it is essential to have a better evaluation of energy storage in water body. For that, a better measurement technique for water depth and water temperature, representative of the area of interest is needed. Finally, in order to match the data sets from different systems, averages over 10 minutes were employed in the present analysis. However, this probably is too short considering the needed steady state condition for application of various approaches to determine fluxes. For the operational measurements, it is probably better to use averaging over a longer

time duration, such as 30 minutes.

Soil moisture measurements by the new TDR sensors were quite successful, with its reliability and accuracy of 2-3% which agrees with the accuracy specified by the manufacturer. The issue that is needed further studies includes the reliability of the probes in the long term measurements. Since these probes are buried within the soil with close to 100% moisture, it is likely to fail more easily than the other sensors. This was not tested in the present study with the data of short time observation.

Overall, the stations were judged suitable for short time, reliable operation in hot, humid area. However, to further increase the reliability in a long term monitoring purposes, a better protection against a heavy rainfall in tropics is judged needed.

Finally, it is probably worth mentioning that some of the findings and experiences of the test operation have been used to modify and improve the stations after the experiment. The modifications made so far to the PAM station include the adoption of the new bandpass algorithm (Horst *et al.*, 1997) mentioned above, a thorough addition of the o-rings to the connectors for better protection against humidity and rainfall, and a replacement of the ATI sonic anemometer with a new Gill sonic anemometer. The change of sonic anemometer was made, despite the higher costs of Gill anemometer, because the ATI sonic is known to require frequent service jobs and to cause problems in a long-term use, while the Gill anemometers have reputation to be a robust system suitable for long- term field use; also the Gill anemometer consumes much smaller electricity (4W approximately) than the ATI (12W). This has reduced the entire energy consumption of PAM system from 26W down to 18W.

Acknowledgments

The experiment was carried out in the framework of GAME-tropics and GAME-AAN, in collaboration with National Research Council of Thailand (NRCT). Mrs.Mathuros Sumipan of NRCT helped us in solving various research as well as practical problems in Thailand. Local support and logistics during the experiment were provided from members of Royal Irrigation Department. Partial financial support came from Asian Pacific Network (APN), and Ministry of Education, Science and Culture of Japan. We would like to thank them all.

Appendix:

A-I. Pre-processing of turbulent data

1. Correction for inclination of the sonic sensor

In the PAM system, turbulence data are stored as set of covariance matrix rather than a set of time series to reduce data amount. The inclinations of sonic anemometer are measured with a clinometer attached to the sonic probe. Five -minute mean values of the rotation angle (a_level, positive clockwise when looked from side of the tower along the boom) and the tilt angle (b_level, positive downward from the horizontal boom, see **Figure A1**). In what follows, the U-component of the wind field corresponds to the direction along the sonic boom (positive from sonic probe to the tower) and V-component the wind from right to left when standing in front of the sonic facing the tower. Finally W-component is positive upward and the three components of U, V, W form a right handed coordinate system. In this coordinate system, the coordinate transformation from tilted system (denoted by U_0, V_0, and W_0) to horizontal one (U, V, and W) can be expressed by the following coordinate transformation matrix, T,

$$\begin{bmatrix} U \\ V \\ W \end{bmatrix} = T \begin{bmatrix} U_0 \\ V_0 \\ W_0 \end{bmatrix} \tag{A1}$$

with

$$T = \begin{bmatrix} \cos(b) & \sin(b)\cos(a) & -\sin(b)\cos(a) \\ 0 & \cos(a) & -\sin(a) \\ \sin(b) & \cos(b)\sin(a) & \cos(b)\cos(a) \end{bmatrix} \tag{A2}$$

where a and b stand for the values of a_level and b_level. This is derived from Axford (1968) by omitting the left wing forwarded angle. By apply-

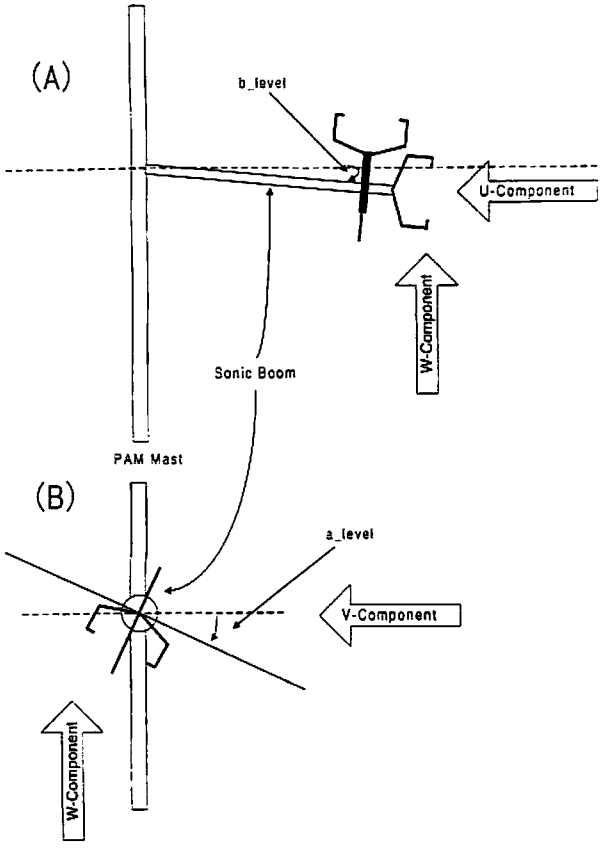

Fig. A1 Definition of wind velocity components U, V, and W, and inclination angles, a_level and b_level. The upper figure (A) indicates the sonic sensor on the sonic boom viewed from the horizontal direction parpendicular to the boom. The lower figure (B) illustrates the anemometer viewed from the direction of the sonic boom stretch looking at PAM mast.

ing (A1)-(A2) to the measured wind speed components by a tilted sonic sensor, it is possible to determine the wind speed field in a horizontal coordinate system. This technique has already been applied to an on-board turbulence measurement over open sea (Tsukamoto *et al.*, 1990) and surface flux measurements in HEIFE project (Tsukamoto *et al.*, 1995).

This transformation means the following equations.

$$U = U_0\cos(b) - V_0\sin(b)\sin(a) - W_0\sin(b)\cos(a) \quad \text{(A3)}$$

$$V = V_0\cos(a) - W_0\sin(a) \quad \text{(A4)}$$

$$W = U_0\sin(b) + V_0\cos(b)\sin(a) + W_0\cos(b)\cos(a) \quad \text{(A5)}$$

This calculations should be directly applied to the mean values of U, V and W, *i.e.*, UM, VM, and WM, respectively. The covariance matrix are transformed as follows from

$$UU = UU_0\cos(b)^2 + VV_0\sin(b)^2\sin(a)^2 + WW_0\sin(b)^2\cos(a)^2 - 2\,UV_0\sin(b)\cos(b)\sin(a) + 2\,VW_0\sin(b)^2\sin(a)\cos(a) - 2\,UW_0\sin(b)\cos(b)\cos(a) \quad \text{(A6)}$$

$$VV = VV_0\cos(a)^2 + WW_0\sin(a)^2 + 2\,VW_0\sin(a)\cos(a) \quad \text{(A7)}$$

$$WW = UU_0\sin(b)^2 + VV_0\cos(b)^2\sin(a)^2 + WW_0\cos(b)^2\cos(a)^2 + 2\,UV_0\sin(b)\cos(b)\sin(a) + 2\,VW_0\cos(b)^2\sin(a)\cos(a) + 2\,UW_0\sin(b)\cos(b)\cos(a) \quad \text{(A8)}$$

$$UV = UV_0\cos(b)\cos(a) - UW_0\cos(b)\sin(a) + VV_0\sin(b)\sin(a)\cos(a) + VW_0\,[\sin(b)\sin(a)^2 - \sin(b)\cos(a)^2] + WW_0\sin(b)\sin(a)\cos(a) \quad \text{(A9)}$$

$$VW = UV_0\sin(b)\cos(a) - UW_0\sin(b)\sin(a) - VV_0\cos(b)\sin(a)\cos(a) + V_0W_0\,[\cos(b)\cos(a)^2 - \cos(b)\sin(a)^2] + W_0W_0\cos(b)\sin(a)\cos(a) \quad \text{(A10)}$$

$$UW = UU_0\sin(b)\cos(a) - UV_0\,[\sin(b)^2\sin(a) - \cos(b)^2\sin(a)] + UW_0\,[\cos(b)^2\cos(a) - \sin(b)^2\cos(a)] - 2\,VW_0\sin(b)\cos(b)\sin(a)\cos(a) - WW_0\sin(b)\cos(b)\cos(a)^2 \quad \text{(A11)}$$

$$UT = UT_0\cos(b) - VT_0\sin(b)\sin(a) - WT_0\sin(b)\cos(a) \quad \text{(A12)}$$

$$VT = VT_0\cos(a) - WT_0\sin(a) \quad \text{(A13)}$$

$$WT = UT_0\sin(b) + VT_0\cos(b)\sin(a) + WT_0\cos(b)\cos(a) \quad \text{(A14)}$$

where the variable such as UW represents covariance of U and W components. Here, terms including higher order "sin(x)" can be neglected assuming small values of inclinations.

2. Derivation of ten-minute mean statistics

In order to allow direct comparison of the results with those obtained from BR system and from SA/IH system, it was necessary to obtain the 10-minute mean statistics from the two sets of 5-minute statistics. Simple mean operation is

sufficient for the mean values such as UM, VM, *etc*. However a careful consideration should be applied to the covariance matrix, because the 5-min statistics include only the information of smaller eddies whose time scale is less than five minutes. For the exact evaluations of 10-min turbulence statistics, the contribution of larger eddies whose time scale is 5-10 minutes, should be included. The following gives an example for the covariance UW.

$$UW_1 = (UW_a + UW_b)/2 \quad \text{(A15)}$$

$$UW_2 = (UM_a \times WM_a + UM_b \times WM_b)/2 - (UM_a + UM_b)/2 \times (WM_a + WM_b)/2 \quad \text{(A16)}$$

UW_1 in (A15) gives normal mean of the two consecutive 5-min statistics UW_a and UW_b, while (A16) produces UW_2, the covariance of UM and WM and this gives the larger eddy contribution. Finally, the 10-min covariance can be obtained as the sum of the two, *i.e.*,

$$UW = UW_1 + UW_2 \quad \text{(A17)}$$

3. Evaluation of vector mean wind direction and wind speed

In the above calculations, the coordinate system for U, V, and W components was based on sonic boom direction. It is often easier and sometimes necessary to adopt the coordinate in the longitudinal and lateral component. The following gives outline of the method of such a rotation of the coordinate system.

Wind direction in U-axis, *i.e.* along the sonic boom direction, is calculated as,

$$d = \tan^{-1}(V/U) \quad \text{(A18)}$$

This is obtained in anti-clockwise direction from upwind direction. It is an opposite sign from normal definition of wind direction. Usual wind direction is calculated as

$$D = 2 \times \pi - d \quad \text{(A19)}$$

Note that this is clockwise from sonic arm direction, which may not necessarily be directed toward north. Vector mean wind speed is calculated as,

$$US = \sqrt{U^2 + V^2} \quad \text{(A20)}$$

Using the mean wind direction during 10 minutes, coordinate transformation to longitudinal component u and lateral component v is applied as follows.

$$u = U\cos(d) + V\sin(d) \quad \text{(A21)}$$

$$v = -U\sin(d) + V\cos(d) \quad \text{(A22)}$$

This is first applied to the mean values of U and V to get mean value of u. Then it is applied to covariance matrix as follows.

$$uu = UU\cos(d)^2 + VV\sin(d)^2 + 2\,UV\sin(d)\cos(d) \quad \text{(A23)}$$

$$vv = UU\sin(d)^2 + VV\cos(d)^2 - 2\,UV\sin(d)\cos(d) \quad \text{(A24)}$$

$$ww = WW \quad \text{(A25)}$$

$$uv = -UU\sin(d)\cos(d) + VV\sin(d)\cos(d) + UV\cos(d)^2 - \sin(d)^2 \quad \text{(A26)}$$

$$uw = UW\cos(d) + VW\sin(d) \quad \text{(A27)}$$

$$vw = -UW\sin(d) + VW\cos(d) \quad \text{(A28)}$$

$$ut = UT\cos(d) + VT\sin(d) \quad \text{(A29)}$$

$$vt = -UT\sin(d) + VT\cos(d) \quad \text{(A30)}$$

$$wt = WT \quad \text{(A31)}$$

The same procedure can be applied for the humidity covariance statistics of uq, vq and wq.

4. Flow inclination correction

Ideally the wind flow should be horizontal and mean value of w should be zero. However, it is not always true and sometimes upflow or downflow is observed, probably due to flow distortion by probe and/or tower or due to inhomogeneity of wind field. This effect should also be considered for a careful determination of fluxes.

The upflow (downflow) angle is obtained as,

$$f = \tan^{-1}(W/US) \quad \text{(A32)}$$

The flow angle can be determined with ensemble average of various wind directions. In the present study, it is determined for each 10 minutes. Then the final coordinate transformation is applied as follows.

$$u = u_0\cos(f) + w_0\sin(f) \quad \text{(A33)}$$

$$w = -u_0\sin(f) + w_0\cos(f) \quad \text{(A34)}$$

and for the covariance matrix,

$$uu = u_0u_0\cos(f)^2 + w_0w_0\sin(f)^2 + 2\,u_0w_0\sin(f)\cos(f) \quad \text{(A35)}$$

$$vv = v_0v_0 \quad \text{(A36)}$$

$$ww = u_0u_0\sin(f)^2 + w_0w_0\cos(f)^2$$

$$-2u_0w_0\sin(f)\cos(f) \quad \text{(A37)}$$

$$uw = (w_0w_0 - u_0u_0)\sin(f)\cos(f) + u_0w_0\,[\cos(f)^2 - \sin(f)^2] \quad \text{(A38)}$$

$$vw = -u_0v_0\sin(f) + v_0w_0\cos(f) \quad \text{(A39)}$$

$$wt = -u_0t\sin(f) + w_0t\cos(f) \quad \text{(A40)}$$

$$wq = -u_0q\sin(f) + w_0q\cos(f) \quad \text{(A41)}$$

where variables with subscript o denote those before flow inclination correction obtained in previous section.

5. Horizontal wind conlamination on the sonic temperature

Temperature derived from sonic anemometer includes a small contamination due to the wind velocity normal to the acoustic path (see *e.g.*, Kaimal and Finnigan, 1994). Since the sonic temperature is usually evaluated by the data from a vertical path, sonic temperature is affected by the horizontal wind. With the knowledge of the horizontal wind velocities, it is possible to remove this contamination. This is automatically carried out in the ATI sonic anemometer of PAM system. In the Kaijo sonic anemometer of SA/IH system, this correction was not applied. This is acceptable because at normal condition, the wind effect becomes significant in temperature measurement at 0.1 degrees C level only when wind speed normal to the path is larger than 5 m/s. Similarly for the flux calculation of H by the eddy correlation method, the correction level can be estimated by equation (B-5) of Kaimal and Gaynor (1991) as 8 W/m² at 5 m/s wind speed. and becomes much larger as wind speed increases. The largest horizontal wind speed recorded during the experiment was as small as 2 m/s.

A-II. Empirical equations to determine the needed variables

The value of ρ can be given, for example, by the following empirical equation (Fairall *et al.*, 1997),

$$\rho = 1 / [287\times(T+273.16)\times(1+0.61q)] \times p \times 100 \text{ kg/m}^3 \quad \text{(A42)}$$

where T is the air temperature in °C, q the specific humidity in kgkg^{-1} and p the atmospheric pressure in hPa. The latent heat of evaporation in Jg^{-1} can be given by an empirical equation such as that of Fritschen and Gay (1979)

$$l = (2.501 - 0.00237\times T)\times 10^3 \text{ Jg}^{-1} \quad \text{(A43)}$$

References

Aoki, M., T. Machimura, Y. Hideshima, N. Obase, M. Wada and T. Satoh (1997) : A data acquisition system for evapotranspiration measurement in remote fields using mobile telephone and small DC generator, *J Agricul. Meteorol.*, 52, in press.

Axford, D.N. (1968) : On the accuracy of wind measurements using an inertial platform in an aircraft, and an example of a measurement of the vertical mesostructure in the atmosphere, *J. Applied Meteorol.*, 7, pp. 645-666.

Brutsaert, W. (1982) : Evaporation Into the Atmosphere, D. Reidel, p. 299, Dordrecht.

Brutsaert, W. (1992) : Stability correction functions for the mean wind speed and temperature in the unstable surface layer, *Geophys. Res. Lett.*, **19**, pp. 469-472.

Businger, J.A. (1988) : A note on the Businger -Dyer Profiles, *Bound.-Layer Meteorol.*, **42**, pp. 145-151.

Dalton, F.N., W.N. Herkelrath, D.S. Rawlins and J.D. Rhoades (1984) : TDR : Simultaneous measurement of soil water content and electrical conductivity with a single prove, *Science*, 224, pp. 989-990.

Dyer, A.J. (1974) : A review of flux-profile relationships, *Bound.-Layer Meteorol.*, 7, pp. 363-372.

Fairall, C.W., E.F. Bradley and D. Rogers (1997) : TOGA-COARE Bulk Flux Algorithm, available at http://www.ncdc.noaa.gov/coare/catalog/data/atmosphere_large_scale/bulk. html.

Fritschen, L.J. and K.W. Gay (1979) : Environmental Instrumentation, Springer-Verlag, p. 215, New York.

Goudie, A. and J. Wilkinson (1977) : The Warm Desert Environment, p. 88, Cambridge.

Högström, U. (1988) : Non-dimensional wind and temperature profiles in the atmospheric surface layer : A re-evaluation, *Bound.-Layer Meteorol.*, 42, pp. 55-78.

Horst, T.W. and S.P. Oncley (1995) : Flux -PAM measurement of scalar fluxes using cospectral similarity. Proceedings of the 9th Symposium on Meteorological Measurements and Instrumentation, 495-500.

Horst, T.W., S.P. Oncley, and S.R. Semmer (1997) : Measurement of water vapor fluxes using capacitance RH sensors and cospectral similarity. Proceedings of the 12th Symposium on Boundary Layers and Turbulence, 360-361.

Kaimal, J.C. and J.J. Finnigan (1994) : Atmospheric Boundary Layer Flows, Oxford Univ. Press. p. 289, New York.

Kaimal, J.C. and J.E. Gaynor (1991) : Another look at sonic thermometry, *Bound.-Layer Meteorol.*, 56, pp. 401-410.

Militzer, J.M., M.C. Michaelis, S.R. Semmer, K.S. Norris, H.W. Horst, S.P. Oncley, A. C. Delany and F.V. Brock (1995) : Development of the prototype PAM III/Flux-PAM surface meteorological station. Proceedings of the 9th Symposium on Meteorological Measurements and Instrumentation.

Stacheder, M. (1996) : Die Time Domain Reflectometry in der Geotechnik, Schr. Angew. Geol. Karlsruhe, p. 170.

Sugita, M. (1996) : Determination of evaporation (1), Lecture Series on Evaportanspiration II, *Hydrology (J. Jpn. Assoc. Hydrol., Sci.)*, 26, pp. 49-56. (in Japanese)

Sugita. M. and W. Brutsaert (1996) : Optimal measurement strategy for surface temperature to determine sensible heat flux from anisothermal vegetation, *Water Resour. Res.* 32(7), pp. 2129-2134.

Topp, G.C., J.L. Davis and A.P. Annan (1980) : Electromagnetic determination of soil water content:Measurements in coaxial transmission lines, *Water Resour. Res.*, 16, pp. 574-582.

Tsukamoto. O., E. Ohtaki, H. Ishida, M. Horiguchi and Y. Mitsuta (1990) : On-Board direct measurements of turbulent fluxes over the open sea, *J. Meteorol. Soc. Japan*, 68, pp. 203-211.

Tsukamoto. O., K. Sahashi and J. Wang (1995) : Heat budget and evapotranspiration at an oasis surface surrounded by desert, *J. Meteorol. Soc. Japan*. 73, pp. 925-935.

Webb, E.K., G.I. Pearman and R. Leuning (1980) : Correction of flux measurements for density effects due to heat and water vapour transfer, *Quat. J. Roy. Met. Soc.*, 106, pp. 85-100.

(Received: Jun. 2, 1997, Accepted: Oct. 23, 1997)